

Breaking the diffraction resolution limit by stimulated emission: stimulated-emission-depletion fluorescence microscopy

Stefan W. Hell and Jan Wichmann

Department of Medical Physics, University of Turku, Tykistökatu 6, 20521 Turku, Finland

Received March 7, 1994

We propose a new type of scanning fluorescence microscope capable of resolving 35 nm in the far field. We overcome the diffraction resolution limit by employing stimulated emission to inhibit the fluorescence process in the outer regions of the excitation point-spread function. In contrast to near-field scanning optical microscopy, this method can produce three-dimensional images of translucent specimens.

Far-field fluorescence light microscopy is a versatile technique for investigating biological specimens. Focused beams are able to penetrate translucent specimens, thus permitting the generation of three-dimensional images of living specimens.¹ Since the research of Abbé it has been considered that the resolution limits of light microscopy based on focusing optics had been reached.² In a recent study³ the possibility of overcoming the classical resolution limit by a factor of 2 was shown by use of two-photon excitation. In this Letter we show how to increase the resolution by a factor of 4.5 by utilizing stimulated emission.

Figure 1 displays the energy levels involved in the excitation and the subsequent emission process of a typical fluorophore.⁴ S_0 and S_1 are the ground and the first excited electronic state, respectively. L_0 is a low vibrational level of S_0 , and L_1 is the directly excited level of S_1 . Similarly, L_2 is the relaxed vibrational level of S_1 , and L_3 is a higher level of S_0 . Figure 2 depicts the setup of our proposed stimulated-emission-depletion (STED) fluorescence scanning microscope. The excitation light generating the $L_0 \rightarrow L_1$ transition originates from a point source consisting of a laser focused onto a pinhole. The point source is imaged into the specimen by the objective lens. The intensity distribution of the excitation light in the focal plane of the lens is determined by diffraction and described by the point-spread function⁵ (PSF) $h_{\text{exc}}(\nu) = \text{const.} |2J_1(\nu)/\nu|^2$. J_1 is the first-order Bessel function, and $\nu = 2\pi r \text{N.A.}/\lambda_{\text{exc}}$ is the optical unit in the focal plane. r is the distance from the focal point, N.A. is the numerical aperture, and λ_{exc} is the wavelength of the excitation light. The excitation PSF $h_{\text{exc}}(\nu)$ is indicated on the right-hand side of Fig. 2. $h_{\text{exc}}(\nu)$ quantifies the probability that an excitation photon arrives at ν and the spatial extent of $h_{\text{exc}}(\nu)$ determines the resolution of a scanning fluorescence microscope.⁵

One possible way to reduce the spatial extent of the $h_{\text{exc}}(\nu)$ is to inhibit the fluorescence in the outer regions of $h_{\text{exc}}(\nu)$. This is equivalent to an increase in resolution. We propose the employment of an additional beam of light, which we call the STED beam,

to inhibit fluorescence. In Fig. 2 the STED beam is emitted from a second laser and split into two beams focused with small lateral offsets $\pm \Delta\nu$ with respect to the excitation beam. If the offset is chosen appropriately ($3 < \Delta\nu < 7$), the intensity distributions of the STED beams in the focal plane, $h_{\text{STED}}(\nu \pm \Delta\nu)$, overlap with the excitation beam on either side. The role of the STED beam is to induce the transition $L_2 \rightarrow L_3$ by stimulated emission and to deplete the excited state before fluorescence takes place. Thus only the innermost region of the main maximum of $h_{\text{exc}}(\nu)$ contributes to the fluorescence signal. The spatial and temporal behaviors of the population probabilities $n_i(\nu, t)$ of the levels L_i ($i = 0, 1, 2, 3$) of the dye are described by a set of coupled differential equations relating the interplay among the absorption, quenching, vibrational relaxation, stimulated emission, and spontaneous emission:

$$\begin{aligned} \frac{dn_0}{dt} &= h_{\text{exc}}\sigma_{01}(n_1 - n_0) + \frac{1}{\tau_{\text{vibr}}}n_3, \\ \frac{dn_1}{dt} &= h_{\text{exc}}\sigma_{01}(n_0 - n_1) - \frac{1}{\tau_{\text{vibr}}}n_1, \\ \frac{dn_2}{dt} &= \frac{1}{\tau_{\text{vibr}}}n_1 + h_{\text{STED}}\sigma_{23}(n_3 - n_2) - \left(\frac{1}{\tau_{\text{fluor}}} + Q\right)n_2, \\ \frac{dn_3}{dt} &= h_{\text{STED}}\sigma_{23}(n_2 - n_3) + \left(\frac{1}{\tau_{\text{fluor}}} + Q\right)n_2 - \frac{1}{\tau_{\text{vibr}}}n_3, \end{aligned} \quad (1)$$

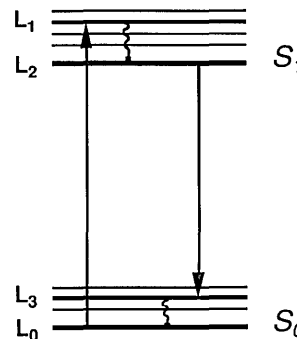


Fig. 1. Energy levels of a typical fluorophore.

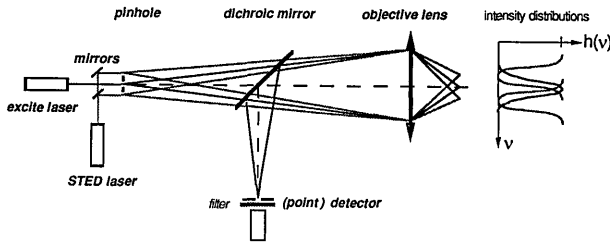


Fig. 2. Principles of a STED fluorescence scanning microscope. An excitation beam and two offset STED beams are focused into the object for excitation and stimulated emission, respectively. The spontaneously emitted light is recorded in a (point) detector. We accomplish imaging by scanning the beams with respect to the object. Two additional STED beams are used for enhancing the lateral resolution in the direction perpendicular to the plane of the scheme. For clarity the lenses for focusing the laser beams into the pinhole plane are not shown.

with $\sum_i n_i = 1$ and $n_0(t = 0) = 1$. τ_{fluor} is the average fluorescence lifetime, and τ_{vibr} is the average vibrational relaxation time for $L_1 \rightarrow L_2$ and $L_3 \rightarrow L_0$. $\sigma_{01}h_{\text{exc}}$ is the rate coefficient for absorption, and $\sigma_{23}h_{\text{STED}}$ is the rate coefficient for stimulated emission from $L_2 \rightarrow L_3$ for $h_{\text{exc}}(\nu)$ and $h_{\text{STED}}(\nu)$, given in terms of photon fluxes. σ_{01} and σ_{23} are the cross sections for the absorptions $L_0 \rightarrow L_1$ and $L_3 \rightarrow L_2$, respectively. Typical values for σ_{01} and σ_{23} range between 10^{-16} and 10^{-17} cm². τ_{fluor} is of the order of 2 ns, and the quenching rate Q is typically 10^8 s⁻¹. With typical lifetimes of $\tau_{\text{vibr}} \approx 1-5$ ps, the vibrational relaxations $L_1 \rightarrow L_2$ and $L_3 \rightarrow L_0$ are 3 orders of magnitude faster than the spontaneous emission $L_2 \rightarrow L_3$.⁴ Because of the dynamic nature of this process it is advantageous to use pulsed lasers with pulses significantly shorter than the average lifetime of L_2 , i.e., pulses in the picosecond range. With an appropriate choice of delay Δt between the pulses, pulsed illumination permits a temporal separation of excitation and stimulated emission. The optimal value of Δt is such that the stimulated-emission pulse arrives as soon as the excitation pulse has left. In this case L_2 is not being populated while stimulated emission is taking place, so that the depletion process of L_2 is very efficient. The stimulated-emission pulses are preferably longer than $\tau_{\text{vibr}} \approx 1-5$ ps since the lifetime of L_3 determines the rate at which L_2 can be depleted.

For pulsed lasers, $h_{\text{STED}}(\nu)$ and $h_{\text{exc}}(\nu)$ are functions of time, and the duration of a Gaussian pulse is quantified by the temporal FWHM $\Delta\tau_{\text{FWHM}}$. Equations (1) were solved numerically for Gaussian pulses $h_{\text{STED}}(\nu)$ of $\Delta\tau_{\text{FWHM}} = 200$ ps $\gg \tau_{\text{vibr}}$. Figure 3 shows how a (spatially and temporally) Gaussian STED-beam pulse leaves depleted areas in an initially uniform distribution of excited molecules $n_2(\nu, t = 0) = 1$. The values of $n_2(\nu)$ are calculated for peak intensities of $h_{\text{STED}}^{\text{peak}} = 3.4, 34, 170,$ and 1300 MW/cm², corresponding to curves a, b, c, and d, respectively. A wavelength of $\lambda_{\text{STED}} = 600$ nm and a cross section σ_{23} of 10^{-16} cm² were assumed. Figure 3 reveals that the depleted area increases in diameter and features increasingly steeper edges

as the intensity of the STED beam is increased. The steep edges of curves c and d permit the sharp limitation of the excitation PSF, as indicated on the right-hand side of Fig. 2. After the STED beam has passed the focal region the majority of the molecules not having undergone stimulated emission are still excited. This is due to the fact that the lifetime τ_{fluor} of L_2 is an order of magnitude larger than the duration of the pulse. The effective PSF of the (nonconfocal) STED fluorescence microscope is given by $h_{\text{eff}}(\nu, \Delta\nu) = h_{\text{exc}}(\nu)n_2(\nu \pm \Delta\nu)$. The function $n_2(\nu \pm \Delta\nu)$ is the normalized population left by two laterally offset STED-beam pulses. Figure 4 displays the PSF for the STED fluorescence microscope, $h_{\text{eff}}(\nu, \Delta\nu = 3.9)$ (curve a), the confocal, $|h_{\text{exc}}(\nu)|^2$ (curve b), and the conventional scanning fluorescence microscope $h_{\text{exc}}(\nu)$ (curve c). The effective PSF was calculated for $h_{\text{STED}}^{\text{peak}} = 1300$ MW/cm² (Fig. 3, curve d). The increase in resolution becomes evident when we compare the FWHM's of the PSF's; 3.2 for the conventional, 2.3 for the confocal, and 0.7 for the STED fluorescence microscopes. Therefore the resolution of the STED is 3.3 and 4.5 times higher than that of the confocal and the conventional fluorescence microscopes, respectively. We have calculated the effective PSF for varying offsets $\Delta\nu$. We found that the resolution increases with decreasing

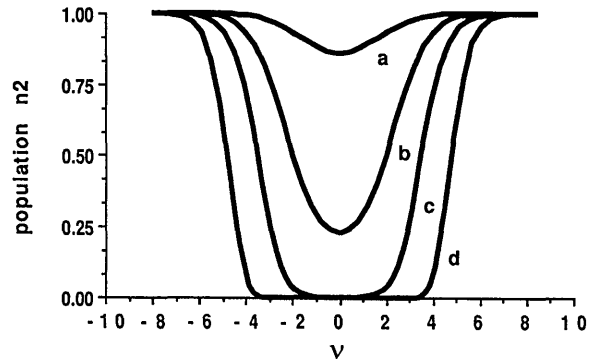


Fig. 3. Population probability $n_2(\nu)$ of L_2 after Gaussian STED-beam pulses of peak intensities of 3.4, 34, 170, and 1300 MW/cm² for curves a, b, c, and d, respectively, have left the focal region. (The computational error of the numerical data is less than 0.1%. These curves and curve a of Fig. 4 have been calculated with a density of 150–200 points per curve.)

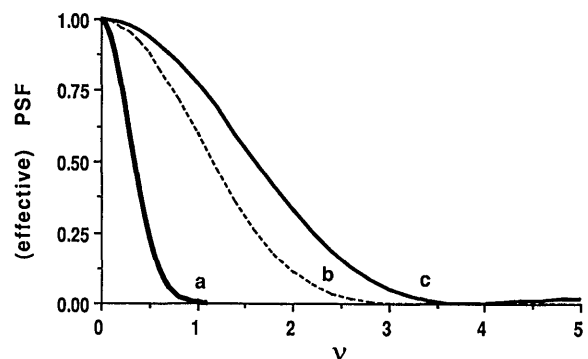


Fig. 4. PSF's for the STED fluorescence microscope with $\Delta\nu = 3.9$ (curve a) and the confocal (curve b) and conventional scanning microscopes in the focal plane.

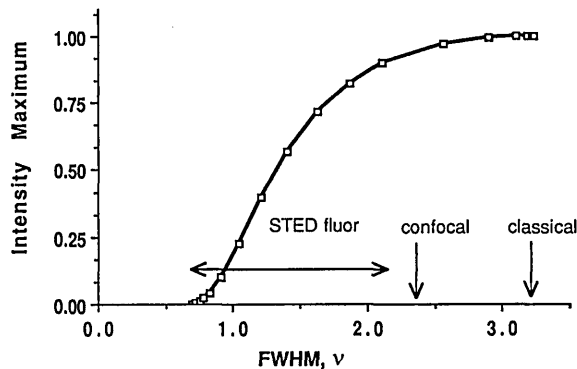


Fig. 5. Intensity maximum versus the FWHM of the effective PSF of the STED fluorescence microscope.

$\Delta\nu$, which brings the beams closer to the focal point. However, the increase in resolution is associated with a reduction in maximum signal strength (Fig. 5). The reason is that the depletion curve (Fig. 3, curve d) is not entirely rectangular. Figure 5 reveals that, for a resolution enhancement of 3, the maximum intensity is approximately 25% that of a conventional microscope. For the conditions specified above the smallest possible FWHM of the effective PSF is 0.68. With a rectangular depletion curve, the resolution could be enhanced to infinity.

A suitable STED laser is a mode-locked dye laser providing picosecond pulses with a repetition rate f of the order of 100 MHz. For biological applications it is of interest to calculate the average power with which the sample is illuminated. The assumed pulse peak power $h_{\text{STED}}^{\text{peak}}$ of 1300 MW/cm² is 3 or-

ders of magnitude less than that used for performing two-photon fluorescence microscopy. The average power is $P_{\text{STED}}^{\text{av}} = h_{\text{STED}}^{\text{peak}} \Delta\tau_{\text{FWHM}} f \pi (0.61\lambda/\text{N.A.})^2$. For $h_{\text{STED};a,b,c,d}^{\text{peak}}$ of Fig. 3, N.A. = 1.4, and $\lambda = 600$ nm, the average power of the STED beams are $P_{\text{STED};a,b,c,d}^{\text{av}} = 0.13, 1.3, 6.5, \text{ and } 50$ mW. The potential of STED fluorescence microscopy is shown in the following example: For the Rhodamine B dye an excitation at 490 nm and a stimulated emission at 600 nm can be assumed. In this case the FWHM of $h_{\text{eff}}(\nu, \Delta\nu = 3.9)$ of a N.A. = 1.4 lens is 50 nm. For a dye with an average emission wavelength of 400 nm, the FWHM is 35 nm. This resolution is based on a genuine reduction of the extent of the PSF in the focal plane and is of the same order as that of scanning near-field light microscopy. The STED fluorescence microscope, however, is able to investigate the space inside translucent specimens and to generate three-dimensional images. The STED fluorescence microscope fundamentally breaks the classical resolution limits and is, to our knowledge, the type of microscope offering the highest resolution in the far field.

References

1. J. Darnell, H. Lodish, and D. Baltimore, *Molecular Cell Biology* (Freeman, New York, 1990), Chap. 4.
2. R. Kopelman and W. Tan, *Science* **262**, 1382 (1993).
3. S. W. Hell, *Opt. Commun.* **106**, 19 (1994).
4. K. H. Drexhage, in *Dye Lasers*, F. P. Schäfer, ed. (Springer-Verlag, Berlin, 1977), p. 144.
5. T. Wilson and C. J. R. Sheppard, *Theory and Practice of Optical Scanning Microscopy* (Academic, London, 1984), p. 47.